Generalized Exclusion Statistics in Astrophysics

Jaime Anguiano Olarra

2023, July, 10th

Abstract

The free ideal gas of excitations following Polychronakos's fractional statistics is explored from a geometrical point of view. The introduction of corrections terms to the ground-state of pure bosons as one already proposed by other authors as well as a generalization of it is also applied and compared to the bare case where this factor is not included. Later, by a change of paradigm, the dependence of curvature on the fractional parameter is inverted into a relation for how the fractional parameter is affected by curvature, and the subsequent influence of this in the probability for the ideal gas to manifest a certain fractional parameter. The distribution of the number of particles and the internal energy is then evaluated for relevant cases under different curvatures in realistic astrophysical conditions. A remarkable twist in the characterization of the level of *fermionicity* over curvature unveils under certain backgrounds.

Keywords: generalized - exclusion - statistics - astrophysics - curvature - anyons

jaimeangola.github@gmail.com

Introduction

The consequences of the statistics obeyed by fields is arguably one of the cornerstones of nature[1] but the proof of its assignment according to spin still relies on unbroken symmetries in a world of broken symmetries. Fractional statistics, the study of excitations which interpolate in between bosons and fermions, was originated in a time when there were no experimental reasons to explore the physics of those particles of the third kind (using Wilczek nomenclature[2]) but has proven useful and sometimes indispensable to explain experimental phenomena such as the fractional quantum Hall effect[3]. Concomitantly, information geometry techniques to analyze spin-statistics has turn into a go-to tool which might not be regarded merely as a mathematical framework to characterize the distributions of many-body problems, but embraced for a full fledged physical interpretation of its outcomes. A paradigmatic example where the crudity of the relation between geometry and information theory manifests is the black hole information paradox: the possible loss of information during black hole evaporation[4]. There, and abstracting and generalizing, in other extended many-body systems whose components are subject, or suspected to be subject, to entanglement, that relation can turn literally physical, reminiscent of the classic figure where the event horizon is depicted as a binary grid [5]. It was in this arena that Bekenstein discovered the area law, which states that the entropy of black holes depends on their surface as we scale the source in contrast with the volume dependence. It was the first time this behavior common for entanglement entropies was found [6, 7]. Fractional statistics quanta, which we will henceforth call anyons, are allowed when one spatial dimension is inhibited, so in our world they are not expected to be found in nature in 3D[8]. Nevertheless the 2D world is the background in many

experiments, e.g. the search of implementing quantum computing in such a promising status as to receive the attention and generous funding of the private sector[2, 9]. Now, this ruling out of an spatial dimension in astrophysical scenarios bring us back to the peculiar environment previously pointed out, that of black holes. The equivalent of AdS_2 [10] geometry in the vicinity of the horizon of an extreme Kerr black hole can be effectively considered two dimensional, hence, conditions for anyons to manifest there could be met[11]. Furthermore, this geometry (known as NHEK for near horizon extreme Kerr)[11, 12], which can be taken as a proper space-time in its own right[11], exhibits a conformal symmetry along *the throat* of the hole that is an interesting sandbox for theoretical and experimental work which might provide the conditions for anyons to arise. The fact that observations so far suggest that supermassive black holes observed in the extremal regime are the rule rather than the exception encourage us to investigate the physics therein. These elements: information geometry, black holes, and exclusion statistics are then brought together here in the aim of building a better understanding of their possible relations.

The paper is organized as follows. In section 1 we review the basics of generalized exclusion statistics bringing in just the relevant equations for our needs dressed in by a succinct presentation. In section 2 we summarize the essential elements of information geometry required for the following. In section 3 the ideal gas of fractional statistics is analyzed as derived from Polychronakos' statistics and also after applying correction terms. Finally the due discussion of the results brings and end.

In the aims of easing the reproducibility of the results of this work, an appendix provides links to the Mathematica notebooks used during the elaboration of the present paper. A second appendix is devoted to an exercise where we take a complete different point of view and we study the behavior of a gas of anyons under the presence of gravity and we apply it to the specific background of a Kerr solution at realistic values of angular momentum. The third and last appendix is devoted to the derivation of the correction to the ground-state for the case of generalized exclusion statistics.

1 Quick review of generalized exclusion statistics

The idea behind fractional statistics, also called generalized exclusion statistics (GES), is answering the unavoidable question of whether there is something else beyond the so different Fermi-Dirac (FD) and Bose-Einstein (BE) statistics. To this, Haldane[13] pioneered the concept of a new interpolating particle inspired by the quasiparticles in the fractional quantum Hall effect [14]. Whereas his article was of utter importance, we will be using our own lower brow version of an approach due to Polychronakos [14, 15].

Look back at the distribution function for the one particle states for the quantum statistics at the limits: $N = \sum_i \frac{1}{e^{\beta(\epsilon_i-\mu)}\pm 1}$ (where the + sign is to be taken for fermions and the negative - for bosons) [16, 17]. In essence, the denominator differs in the sign of an additive constant of unit value. The positive sign disfavors the probability whereas the negative sign is probability enhancing. We can naively replace them altogether for a parameter, which we will be calling g, that takes on real values on the whole interval $[-1, 1]$ and not only on its boundary. This is the foundation for our anyons. Particles obeying these statistics are said to be ruled by the general exclusion principle (which reduces to Pauli's in the case of $g = 1$). We see that the classical ideal gas is obtained when g equals 0.

The next stop in our summary comes from Wu's seminal paper[18], where he developed the statistical mechanics of these particles providing the Helmholtz potential as well as the entropy in general cases as well as for the gas of free particles in particular. Later, Nayak and Wilczek[14] elaborated on the previous works providing virial coefficients resorting to the Sommerfeld expansion[14] discovering an interesting duality: the

exact behavior of anyons with parameter g and $1/g$. A modified version of this expansion was devised and used later by Aoyama[19] to compute the heat capacity of an ideal anyon gas and, along the way, he found a closed form for the distribution function for values of g which are inverse of a positive integer greater than one. A decade and a half later, Mirza and Mohammadzadeh[20] computed, from information geometry, the curvature for the main implementations of anyonic particles.

For broader insight in fractional statistics, see [8]. Before leaving this section it is worth reminding that the different implementations of fractional statistics don't fully agree in all their results as for example happens with the third virial coefficient of the ideal anyon gas which is radically different for statistics *a la* Polychronakos or *a la* Haldane[8][1].

2 Even quicker review of Information Geometry

"Information geometry is a method of exploring the world of information by means of modern geometry"[21]. The whole idea grounding this discipline can also be stated as an attempt to answer a question: can we visualize the difference in between two statistical distributions as a distance between them in some space?. The birth of a new branch of mathematics arouse from thereof starting the incursion of differential geometry machinery, and later on of topology, on the realm of statistics. In particular by use of the Fisher-Rao metric[21, 22, 23], the differential geometry of the space of distribution functions is analyzed. From the works pioneered by Weinhold, and more influentially, by Ruppeiner, who used an entropy representation bridging the gap with Shannon's theory, Janyszek[24] arrived at the expression for the metric of the parameter space in terms of the partition function[16][25] which has been presented earlier in detail in many references ([25] being suggested) and in the present work it is assumed without proof.

$$g_{\mu\nu} = \frac{\partial^2 \log(Z)}{\partial\lambda^\mu \partial\lambda^\nu} \tag{1}$$

Z is the partition function of the system and λ^μ and λ^ν are Lagrange multipliers of the Legendre transform of the entropy for the interested representation and physically they embed the intensive variables constrained by the problem. We will be working with the grand canonical ensemble, that so, the parameters μ,ν take on two values, these are $\lambda^1 = \beta = \frac{1}{T}$ and $\lambda^2 = \gamma = -\frac{\mu}{T}$, being T the temperature of the system and in the last equality μ is the chemical potential and not an index (explicitly: it has nothing to do with the index appearing in the metric). We implicitly work with T representing energy with no need for Boltzmann's constant. Our manifold is then two dimensional. The scalar curvature can be computed from (where the inessential factor 2 comes as a convention-dependant normalization and can be ignored)[25]:

$$R = 2\frac{\begin{vmatrix} g_{\beta\beta} & g_{\gamma\gamma} & g_{\beta\gamma} \\ g_{\beta\beta,\beta} & g_{\gamma\gamma,\beta} & g_{\gamma\gamma,\beta} \\ g_{\beta\beta,\gamma} & g_{\gamma\gamma,\gamma} & g_{\gamma\gamma,\gamma} \end{vmatrix}}{\begin{vmatrix} g_{\beta\beta} & g_{\beta\gamma} \\ g_{\gamma\beta} & g_{\gamma\gamma} \end{vmatrix}^2} \tag{2}$$

More conveniently, and henceforth, we will use the fugacity $z = e^{-\gamma}$ instead of γ. Having geared up ourselves

[1]Note: the term g-ons is widely used in literature and in deed it is more appropriate for the particles described here which come from Polychronakos' formulation, also named new fractional statistics. Even if there are sometimes subtle and sometimes greater differences in between the two, we use the term anyons as when coming into the realm of gravitation it may be confused with the much older term for the quanta of geometrodynamics known as geons

with the tools we needed from information geometry we end this section. [22] is a suggested monograph on this subject.

3 The Geometry of Generalized Exclusion Statistics

Our starting point will be the direct and comprehensive work by Mirza and Mohammadzadeh[20] who surveyed the most relevant cases[2]. For brevity anyons, instead of an ideal gas of anyons will be frequently used when no possible confusion may arise. Let σ represent the power of the energy of the single particle states in the dispersion relation which we assume to take the form: $\epsilon = A \cdot p^{\sigma}$[20, 25, 26, 27], where A is an overall constant that comes from the density of states for particles in a large box in D dimensions in the continuous limit (or whatever other selected way for building the density of states function, in any case this is not very relevant as A will drop out of the calculation) which is: $G(\epsilon) = \frac{A^D \epsilon^{\frac{D}{\sigma}-1}}{\Gamma\left(\frac{D}{2}\right)}$

The density of states above, applied to the distribution of section 1. gives the following expressions:

$$U = \frac{A^D \beta^{-\frac{D}{\sigma}-1} \Gamma(\frac{D}{\sigma}+1) Li_{\frac{D}{\sigma}+1}(z-2\rho z)}{(1-2\rho)\Gamma\left(\frac{D}{2}\right)} \tag{3}$$

$$N = \frac{A^D \beta^{-\frac{D}{\sigma}} \Gamma\left(\frac{D}{\sigma}\right) Li_{\frac{D}{\sigma}}(z-2\rho z)}{(1-2\rho)\Gamma\left(\frac{D}{2}\right)} \tag{4}$$

$$F = -\frac{\sigma A^D \beta^{-\frac{D}{\sigma}} \Gamma\left(\frac{D+\sigma}{\sigma}\right) Li_{\frac{D+\sigma}{\sigma}}(z-2z\rho)}{D(1-2\rho)\Gamma\left(\frac{D}{2}\right)} \tag{5}$$

According to [20], the domain of the polylogarithm introduces a mathematical singular behavior when it is evaluated at $z - 2\rho z = 1$, hence, for any fractional parameter ρ, there must be a divergence of the curvature at the critical value $z_c = \frac{1}{1-2\rho}$. If we admit this argument, then we should really consider the inequality: $z - 2\rho z \geqslant 1$ as all those values would leak away of the function domain as we will show later.

The expressions for the internal energy (3) and the number of particles (4) can be found in [20]. The expression for the free energy was obtained by integration from (3) with respect to β. It follows that we readily get the metric in the Polychronakos statistics by use of (3) and (4) in (1):

$$g_{\mu\nu} = \begin{pmatrix} g_{\beta\beta} & g_{\beta\gamma} \\ g_{\beta\gamma} & g_{\gamma\gamma} \end{pmatrix} = \begin{pmatrix} -\frac{A^D \beta^{-\frac{D}{\sigma}-2}\Gamma\left(\frac{D}{\sigma}+2\right) Li_{\frac{D+\sigma}{\sigma}}(z-2z\rho)}{(2\rho-1)\Gamma\left(\frac{D}{2}\right)} & -\frac{A^D \beta^{-\frac{D+\sigma}{\sigma}}\Gamma\left(\frac{D+\sigma}{\sigma}\right) Li_{\frac{D}{\sigma}}(z-2z\rho)}{(2\rho-1)\Gamma\left(\frac{D}{2}\right)} \\ -\frac{A^D \beta^{-\frac{D+\sigma}{\sigma}}\Gamma\left(\frac{D+\sigma}{\sigma}\right) Li_{\frac{D}{\sigma}}(z-2z\rho)}{(2\rho-1)\Gamma\left(\frac{D}{2}\right)} & -\frac{A^D \beta^{-\frac{D}{\sigma}}\Gamma\left(\frac{D}{\sigma}\right) Li_{\frac{D}{\sigma}-1}(z-2z\rho)}{(2\rho-1)\Gamma\left(\frac{D}{2}\right)} \end{pmatrix} \tag{6}$$

The corresponding covariant derivative is:

$$D_\mu = g^{\mu\varepsilon}\left(-g_{\zeta\delta}\Gamma^{\zeta}_{\alpha\varepsilon} - g_{\alpha\zeta}\Gamma^{\zeta}_{\delta\varepsilon} + (\partial g)_{\varepsilon\alpha\delta}\right) \tag{7}$$

and the scalar curvature matrix[25]:

[2] In that paper, the authors chose to reparametrize the fractional parameter as to match the range of the other two statistics in their article, namely: Haldane's and Gentile's. A problem arising from their reparametrization is that both the energy and the number of particles, as well as the magnitudes derived from them, they all become singular for $\rho = 1/2$. We circumvent this by evaluating on sufficiently adjacent values to it as to avoid these coordinate divergences. These close-to-but-not-1/2 values will be 0.499 and 0.501 unless a greater difference is needed (0.489 or so sometimes is mandated to be able to plot results)

$$\begin{pmatrix} g_{\beta\beta} & g_{\gamma\gamma} & g_{\beta\gamma} \\ g_{\beta\beta,\beta} & g_{\gamma\gamma,\beta} & g_{\beta\gamma,\beta} \\ g_{\beta\beta,\gamma} & g_{\gamma\gamma,\gamma} & g_{\beta\gamma,\gamma} \end{pmatrix} = \begin{pmatrix} -\frac{A^D\beta^{-\frac{D}{\sigma}-2}\Gamma\left(\frac{D}{\sigma}+2\right)Li_{\frac{D+\sigma}{\sigma}}(z-2z\rho)}{(2\rho-1)\Gamma\left(\frac{D}{2}\right)} & -\frac{A^D\beta^{-\frac{D}{\sigma}}\Gamma\left(\frac{D}{\sigma}\right)Li_{\frac{D}{\sigma}-1}(z-2z\rho)}{(2\rho-1)\Gamma\left(\frac{D}{2}\right)} & -\frac{A^D\beta^{-\frac{D+\sigma}{\sigma}}\Gamma\left(\frac{D+\sigma}{\sigma}\right)Li_{\frac{D}{\sigma}}(z-2z\rho)}{(2\rho-1)\Gamma\left(\frac{D}{2}\right)} \\ \frac{A^D\beta^{-\frac{D}{\sigma}-3}\Gamma\left(\frac{D}{\sigma}+3\right)Li_{\frac{D+\sigma}{\sigma}}(z-2z\rho)}{(2\rho-1)\Gamma\left(\frac{D}{2}\right)} & \frac{A^D\beta^{-\frac{D+\sigma}{\sigma}}\Gamma\left(\frac{D+\sigma}{\sigma}\right)Li_{\frac{D}{\sigma}-1}(z-2z\rho)}{(2\rho-1)\Gamma\left(\frac{D}{2}\right)} & \frac{A^D\beta^{-\frac{D}{\sigma}-2}\Gamma\left(\frac{D}{\sigma}+2\right)Li_{\frac{D}{\sigma}}(z-2z\rho)}{(2\rho-1)\Gamma\left(\frac{D}{2}\right)} \\ \frac{A^D\beta^{-\frac{D}{\sigma}-2}\Gamma\left(\frac{D}{\sigma}+2\right)Li_{\frac{D}{\sigma}}(z-2z\rho)}{(2\rho-1)\Gamma\left(\frac{D}{2}\right)} & \frac{A^D\beta^{-\frac{D}{\sigma}}\Gamma\left(\frac{D}{\sigma}\right)Li_{\frac{D}{\sigma}-2}(z-2z\rho)}{(2\rho-1)\Gamma\left(\frac{D}{2}\right)} & \frac{A^D\beta^{-\frac{D+\sigma}{\sigma}}\Gamma\left(\frac{D+\sigma}{\sigma}\right)Li_{\frac{D}{\sigma}-1}(z-2z\rho)}{(2\rho-1)\Gamma\left(\frac{D}{2}\right)} \end{pmatrix} \tag{8}$$

The scalar curvature is then given by:

$$R = -\frac{(2\rho-1)\Gamma\left(\frac{D}{2}\right)\beta^{D/\sigma}\Gamma\left(\frac{D}{\sigma}+2\right)\Gamma\left(\frac{D}{\sigma}\right)\Gamma\left(\frac{D+\sigma}{\sigma}\right)\left(Li_{\frac{D}{\sigma}-1}(z-2z\rho)Li_{\frac{D}{\sigma}}(z-2z\rho)^2+\left(Li_{\frac{D}{\sigma}-2}(z-2z\rho)Li_{\frac{D}{\sigma}}(z-2z\rho)-2Li_{\frac{D}{\sigma}-1}(z-2z\rho)^2\right)Li_{\frac{D+\sigma}{\sigma}}(z-2z\rho)\right)}{\left(\Gamma\left(\frac{D+\sigma}{\sigma}\right)^2Li_{\frac{D}{\sigma}}(z-2z\rho)^2-\Gamma\left(\frac{D}{\sigma}+2\right)\Gamma\left(\frac{D}{\sigma}\right)Li_{\frac{D}{\sigma}-1}(z-2z\rho)Li_{\frac{D+\sigma}{\sigma}}(z-2z\rho)\right)^2} \tag{9}$$

These general results are now applied to different cases we are interested in and compared to the limits of FD and BE distributions.

3.1 The 3D non-relativistic case:

The 3D case for the extremes of the fractional parameter, Bose-Einstein and Fermi-Dirac distributions, where reviewed recently[25], where for the case of bosons it was argued that much of the misunderstanding of the physical interpretation of the previous results by other authors[20], was due to the fact that the problem had been wrongly posed *ab initio*. The argument in this recent paper was that the continuous approximation, assigning no particles to the ground-state, had to be corrected to properly describe the low temperature limit. As we are dealing with particles of a third kind, we can take advantage of this fact and freely track their steps in an unified view, not only on the boundary of the fractional parameter window, but in all its range both in what we call the bare case, where no correction is applied and after that term is applied. Note that for the correction to be meaningful, the bosons need to be massive. The correction to the ground-state cannot be applied to massless excitations like photons and phonons. This is implicit in the use of the grand canonical partition function which assumes a conserved number of particles. If the anyons considered could transient over different values of their character (adjusting individually or collectively their level of *fermionicity*), the number of particles could not be a sufficiently strong constrain and the system should be studied as a mixture. Besides this, the problem of assigning the value for the curvature to the ground-state remains. The correction chosen by Cafaro and Pessoa grants that it will be zero (flatness). It could be another constant value not necessarily zero and it could be that it has different local minima or take many other forms. Anyway we will see this problem would need to be attacked with a different correction term.

For ease of direct comparison with the results of Cafaro and Pessoa we will be closely follow their sampling space for the different parameters.

3.1.1 From the bare metric

By setting the appropriate values in (6) the metric is found to be:

$$g_{\mu\nu}^{[D3\sigma2]} = \begin{pmatrix} \frac{15Li_{\frac{5}{2}}(z-2z\rho)}{\beta^{7/2}(4-8\rho)} & \frac{3Li_{\frac{3}{2}}(z-2z\rho)}{\beta^{5/2}(2-4\rho)} \\ \frac{3Li_{\frac{3}{2}}(z-2z\rho)}{\beta^{5/2}(2-4\rho)} & \frac{Li_{\frac{1}{2}}(z-2z\rho)}{\beta^{3/2}(1-2\rho)} \end{pmatrix} \tag{10}$$

Where we introduced the superscript $[Dd\sigma s]$ to indicate the dimension d and power of momentum s. The

scalar curvature matrix is:

$$\begin{pmatrix} g_{\beta\beta} & g_{\gamma\gamma} & g_{\beta\gamma} \\ g_{\beta\beta,\beta} & g_{\gamma\gamma,\beta} & g_{\beta\gamma,\beta} \\ g_{\beta\beta,\gamma} & g_{\gamma\gamma,\gamma} & g_{\beta\gamma,\gamma} \end{pmatrix}_{[D3\sigma 2]} = \begin{pmatrix} \frac{15Li_{\frac{5}{2}}(z-2z\rho)}{\beta^{7/2}(4-8\rho)} & \frac{Li_{\frac{1}{2}}(z-2z\rho)}{\beta^{3/2}(1-2\rho)} & \frac{3Li_{\frac{3}{2}}(z-2z\rho)}{\beta^{5/2}(2-4\rho)} \\ -\frac{105Li_{\frac{5}{2}}(z-2z\rho)}{2\beta^{9/2}(4-8\rho)} & -\frac{3Li_{\frac{1}{2}}(z-2z\rho)}{2\beta^{5/2}(1-2\rho)} & -\frac{15Li_{\frac{3}{2}}(z-2z\rho)}{2\beta^{7/2}(2-4\rho)} \\ \frac{15(2\rho z-z)Li_{\frac{3}{2}}(z-2z\rho)}{\beta^{7/2}(4-8\rho)(z-2\rho z)} & \frac{(2\rho z-z)Li_{-\frac{1}{2}}(z-2z\rho)}{\beta^{3/2}(1-2\rho)(z-2\rho z)} & \frac{3(2\rho z-z)Li_{\frac{1}{2}}(z-2z\rho)}{\beta^{5/2}(2-4\rho)(z-2\rho z)} \end{pmatrix} \quad (11)$$

Leading us to the scalar curvature:

$$R = -\frac{20\beta^{3/2}(2\rho-1)\left(Li_{\frac{1}{2}}(z-2z\rho)Li_{\frac{3}{2}}(z-2z\rho)^2 + \left(Li_{-\frac{1}{2}}(z-2z\rho)Li_{\frac{3}{2}}(z-2z\rho) - 2Li_{\frac{1}{2}}(z-2z\rho)^2\right)Li_{\frac{5}{2}}(z-2z\rho)\right)}{\left(3Li_{\frac{3}{2}}(z-2z\rho)^2 - 5Li_{\frac{1}{2}}(z-2z\rho)Li_{\frac{5}{2}}(z-2z\rho)\right)^2} \quad (12)$$

The metric determinant appears as the denominator in the Ricci scalar so it is worth to check its behavior. We obtain for different values of the fractional parameter, for different values it is shown in Fig. 1.

Computing the curvature through (12) we obtain modest positive values for the bosonic sector ($0 < \rho < 0.5$) and observe their decay towards flatness as the fractional parameter approaches $1/2$, a frontier where once crossed, curvature turns negative, but almost flat, to keep negative but dimly increasing in absolute value in the fermionic sector ($0.5 < \rho < 1$). The dependence on fugacity in this range seems weak. Regarding temperature, the bosonic sector increases its curvature with it and the fermionic sector drifts into values more and more negative with it, exposing a somewhat symmetric behavior but of opposite sign.

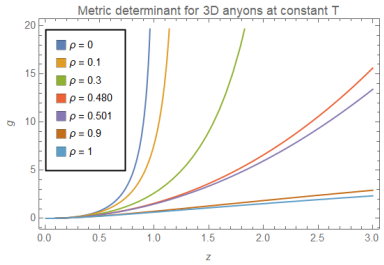

Figure 1: The determinant of the metric as a function of fugacity for a set of different fractional parameter values.

Consistently we arrive at the same results when line plots are used as was done in [25] for bosons Fig. 2. There is no new information in Fig. 3. but the different representation eases the reading. Reducing the temperature reduces the curvature and for low fugacities the absolute value of curvature is almost fugacity independent for all values of the statistical parameter being almost flat for borderline anyons $\rho \sim 1/2$ (classical limit).

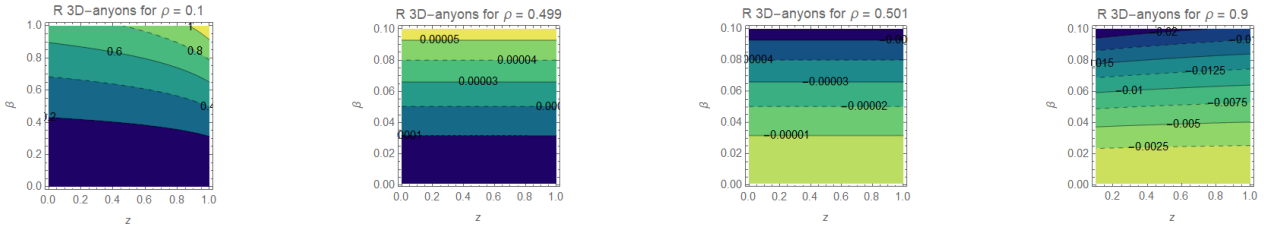

Figure 2: Contour plots of curvature for a set of fractional parameter values ranging from the close bosonic sector ($\rho \sim 0$) reaching to the close fermionic sector ($\rho \sim 1$).

When we turn our attention to the curvature as a function of the fractional parameter of given value of z for which we observe a dull behavior and a smooth transition at the $\rho = 1/2$ point as shown in Fig. 4.

This is not all to the problem. As mentioned above, Mirza and Mohammadzadeh[20] noticed that for any given value of ρ differing from unity, the curvature would be singular at a certain critical value of the fugacity. Fig. 5 and Fig. 6 show a diverging curvature as predicted by they, it doesn't fully blow up in the plots although neither it comes back to lower values, it simply rises up to a certain level just to vanish then

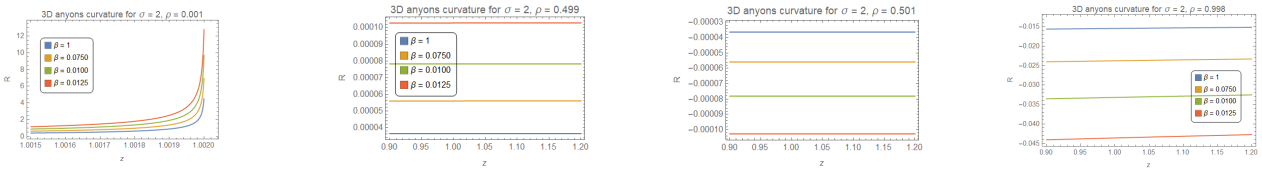

Figure 3: Curvature for a set of fractional parameter values ranging from the close bosonic sector ($\rho \sim 0$) reaching to the close fermionic sector ($\rho \sim 1$)

onward, coinciding with our interpretation that the critical fugacity should not be seen as a point singularity but as branch cut. Another feature that we can infer from the these plots is that there seems to be an alternating pattern in the maxima of the curvature for adjacent values of the fractional parameter suggesting that even if the real behavior (analytically) is asymptotic to infinite curvature, the rates at which this achieved might be different, something we won't dwell into in the present work. Nevertheless from this results, we agree with [20], at these values of fugacity and fractional parameter curvature blows up. Whether this means that condensation or a phase transition takes place is still debated[25] (very recently argued against in [28, 29]). In any case the correction to the ground-state that effectively works for pure BE, cannot avoid this.

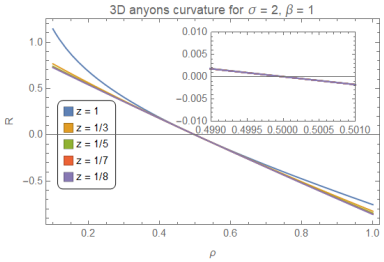

Figure 4: Curvature in terms of the fractional parameter for a different values in the low limit of fugacity.

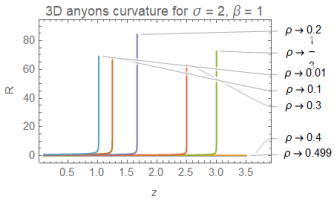

Figure 5: Curvature as a function of fugacity for different values of the fractional parameter in the bosonic sector. We observe the behavior of phase transition first described in [20]

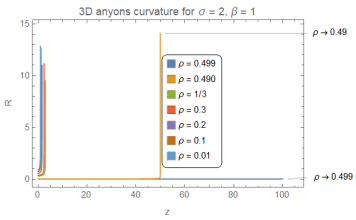

Figure 6: Curvature as a function of fugacity for different values of the fractional parameter in the bosonic sector.

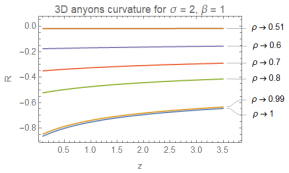

Figure 7: Fermionic sector.

The fermionic sector shows no divergence and as we leave the classical limit ($\rho \sim 0.5$) and we cruise to the pure fermions. As depicted in Fig. 7, by contrast, in the fermionic sector there are no divergences. The borderline cases are almost flat, and so they keep all the way up to very high levels of *fermionicity*. 3D plots in the (z, ρ, R) space are shown in Fig 8.

The singular behavior of R can be easily perceived. Remember that this is really a continuous barrier and that unless ρ or z should be of discrete nature, the appearance of these spikes are an artifact due to the sampling in the construction of the plots. As we travel closer to the fermionic sector, but while remaining in the bosonic sector, higher fugacities are needed for this leaps of curvature to happen. In the fermionic sector, as already pointed out[20] none of this type of singularities arise. There is no BE-phase-transition-like in the fermionic sector. What would happen if we consider the correction to the ground-state?.

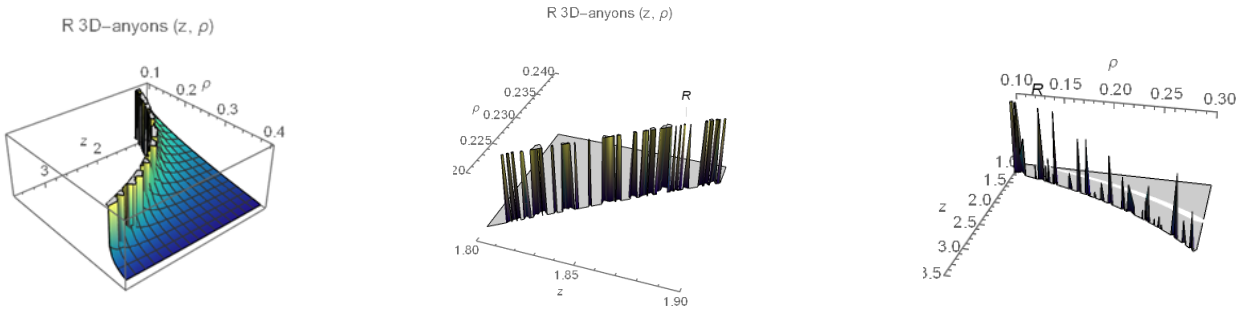

Figure 8: 3D plots in the (z, ρ, R) space show the rim exhibited when the condition predicted[20] is met. Sampling different ranges of the fractional parameter explicitly show that the structure is really that of a continuous cut as long as ρ and z take on continuous values

3.1.2 Under the correction to the generalized exclusion statistics ground-state

The correction introduced by Cafaro and Pessoa[25] is: $N_0 = \frac{1}{\frac{1}{z}-1}$, an additive term to the number of particles (4). This correction term affects the metric in the entry for the double differentiation of the partition function with respect to γ, the wrap of the chemical potential, which we dressed up with an exponential map to another function, fugacity, in the previous subsection. As it is manifest and already explained, the independence on the fractional parameter is a backdoor for the singular behaviour at the matching condition noted by Mirza and Mohammadzadeh. A possible correction for the case of Gentile statistics which would take the form[3]:

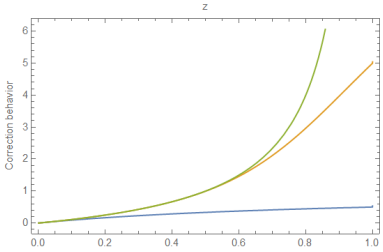

Figure 9: Correction term for Gentile's statistics (blue: pure fermions, orange: ten particles per state, green: 1000 particles per state)

$$N_0 = -\frac{e^{-\gamma}\left(-\frac{\left(e^{-\gamma}\right)^{\frac{1}{\rho}+1}}{\rho} + \left(\frac{1}{\rho}+1\right)\left(e^{-\gamma}\right)^{1/\rho} - 1\right)}{\left(e^{-\gamma}-1\right)\left(\left(e^{-\gamma}\right)^{\frac{1}{\rho}+1} - 1\right)} \tag{13}$$

Where Gentile's maximum allowed occupation number per state has been mapped to the inverse of the fractional parameter here[4].

The behavior of the correction term for GES for different values of the fractional parameter and fugacities is depicted in Fig. 9.

For completeness we try this using pure Gentile's statistics for which closed forms for the internal energy and number of particles were already provided in [20], from which we obtain the metric and the curvature following the procedure of the previous section.

The respective results (Fig. 10 for the Polychronako's metric and Fig. 11 for the Gentile's metric cases respectively) unexpectedly suggest that the correction doesn't suit as well for Gentile's case as for more general

[3]Its derivation can be found in Appendix 3

[4]Even if this term was tailored for Gentile's statistics, we see no reason by it should not work too for Polychronakos' statistics

Polychronakos's statistics. This is probably due to the simpler nature of the Polychronakos' representation of the internal energy and number of particles which involves a single polylogarithm for each, whether Gentile's involves more complex expressions tangling two of those functions for each of those variables. In this later statistics, the correction factor severely affects the determinant which now not only keeps on diverging as we approach $z = 1$ but for very low fractional parameter values the anomalous behavior extends to a larger range of fugacities.

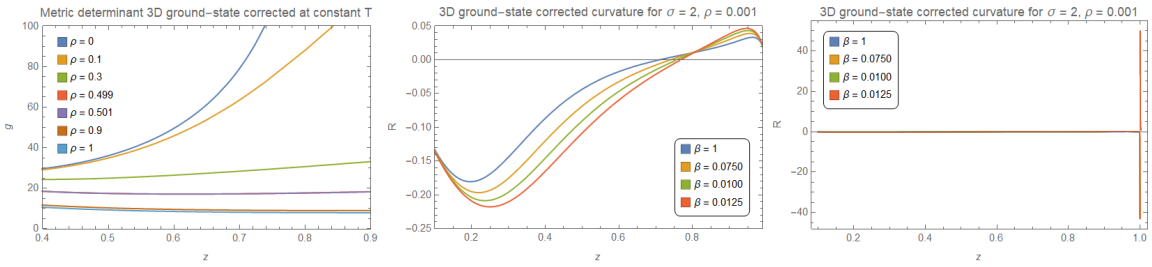

Figure 10: (Left) Metric determinant and curvature after applying the correction for Gentile's statistics applied to the Polychronakos's metric. (Center) The correction seems to tame the pole at z = 1 if we restrict ourselves to values close to it, notice we are approaching $z = 1$ from the left but nevertheless not reaching that value. If we actually step on it we see it blows up (right)

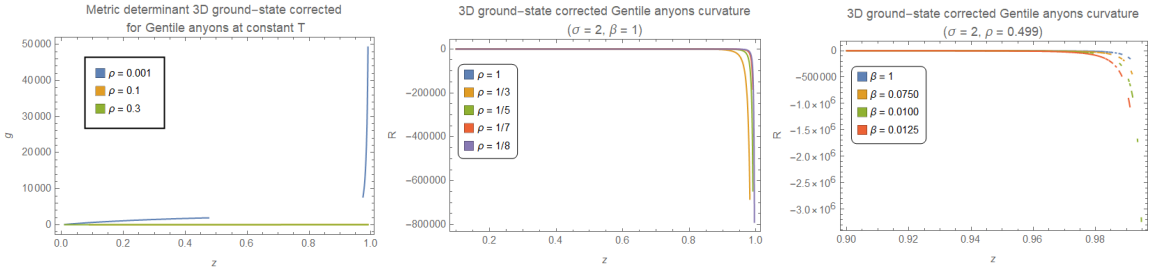

Figure 11: (Left) Metric determinant and curvature after applying the correction for Gentile's statistics to the Gentile's statistics metric. (Center) The curvature for the non-relativistic case as a function of fugacity for different values of the fractional parameter. Right: curvature as a function of fugacity for different temperatures on the far end of the bosonic sector.

We want to close this section mentioning one obvious correction term that we did not mention which regularizes all the singularities but the one at zero fugacity, it is so trivial that it is easy to miss. It uses the matching condition referred above[20]. The singularities arise for the values that obey (in the limit of the range explained earlier): $z - \frac{1}{1-2\rho} = 0$, giving us the zeros we want for the denominator of our correction, which now takes the form:

$$N_0 = \frac{1}{z - \frac{1}{1-2\rho}} \tag{14}$$

Subtraction of this term will remove the infinities coming from the matching condition. This term still has a coordinate singularity at $\rho = 1/2$, which we know it is not physical and can be skipped by just evaluating close to it. Although mathematically correct, the physics of this term alone seem to be wrong as it is inversely proportional to the fugacity. One way out of this for making it reasonable would be to consider it as a signal of being in states out of equilibrium.

Discussion

In the first part we built the structure to analyze the curvature of Polychronakos statistics, extending the previous work by Mirza and Mohammadzadeh[20] and Cafaro and Pessoa[25] providing the metric, the scalar curvature matrix and the Helmholtz free energy and we also clarified some points of the first of these works. Following the idea of introducing a correction to the Bose-Einstein ground-state pioneered by Cafaro and Pessoa[25] we studied the effects of including such a term to the case of generalized exclusion statistics and observed the failure of the terms proposed so far to effectively regularize the divergent behavior of the curvature at certain values of fugacity. This was not without profit, as along the way we realized of something that should had been obvious in hindsight, that searching for these correction terms will be an easier task in the case of Polychronakos' statistics. More work on this will be done in the future. As is seen in the appendix 2, if we explore the consequences of taking literally the maps obtained for the fractional parameter in terms of curvature as a one to one relation, we can invert those to obtain the fractional parameter in terms of curvature, temperature and fugacity. This allows us to observe how the fractional parameter and resulting distribution of the number of particles and internal energy would behave for different values of curvature. Furthermore, we find that the main characterization linking positive curvature to bosons and negative curvature to fermions can be turn upside down under certain backgrounds. Before we leave, we would also like to comment what we have omitted. We assumed the fractional parameter interpolates only and not extrapolates fermions and bosons. That's the reason behind the cutoffs in the 3D plots, for example. Actually the mathematics involved allows for fractional parameters to the left of 0 and beyond 1 along the real line. The fact that the fractional parameter and the number of particles for anyons are sensible to the underlying topology as to suffer severe restrictions on their values(see [8], last chapter), just as we have seen here and also expressed through the internal energy, could serve as a way to probe this last by means of experimentally studying their phase transitions. This calls for experimental setup designs which have not been subject of any try to devise here. Finally, we neglected too the nourishment of a reliable piecewise function of ρ (β, z, R) arranged to cover the full map of values. Being the relation of curvature-statistics a topic of major concern[30] in physics in longstanding undergoing research we are sure this will be done elsewhere.

Acknowledgments

The author wants to express his gratitude to Dr. Pedro Pessoa for useful comments and revision of this manuscript. This paper makes use of the Black Hole Perturbation Toolkit[31]

References

[1] Ian Duck and E C G Sudarshan. *Pauli and the Spin-Statistics Theorem*. WORLD SCIENTIFIC, 1998. DOI: 10.1142/3457. URL: https://doi.org/10.1142/3457.

[2] Frank Wilczek. *Quanta of the Third Kind: Anyons*. 2021 CAP Herzberg Memorial Public Lecture, 2021. [Online]. 2021.

[3] Ady Stern. "Anyons and the quantum Hall effect - a pedagogical review". In: (2007). DOI: 10.48550/ARXIV.0711.4697. URL: https://arxiv.org/abs/0711.4697.

[4] Robert M. Wald. *Quantum Field Theory in Curved Space-Time and Black Hole Thermodynamics*. Chicago Lectures in Physics. Chicago, IL: University of Chicago Press, 1995. ISBN: 978-0-226-87027-4.

[5] John Archibald Wheeler. *A journey into gravity and spacetime*. eng. Scientific American Library series ; no. 31. New York: Scientific American Library, 1990. ISBN: 0716750163.

[6] Jacob D. Bekenstein. "Black Holes and Entropy". In: (2019), pp. 307–320. DOI: 10.1142/9789811203961_0023. URL: https://doi.org/10.1142/9789811203961_0023.

[7] Javier Rodriguez-Laguna et al. "More on the rainbow chain entanglement, space-time geometry and thermal states". In: *Journal of Physics A: Mathematical and Theoretical* 50.16 (Mar. 2017), p. 164001. DOI: 10.1088/1751-8121/aa6268. URL: https://doi.org/10.1088/1751-8121/aa6268.

[8] Avinash Khare. *Fractional Statistics and Quantum Theory*. WORLD SCIENTIFIC, 2005. DOI: 10.1142/5752.

[9] Liam Tung. *Microsoft just upped its multi-million bet on quantum computing*. 2017.

[10] Daniel Kapec and Alexandru Lupsasca. "Particle motion near high-spin black holes". In: (2019). DOI: 10.48550/ARXIV.1905.11406. URL: https://arxiv.org/abs/1905.11406.

[11] Alexandru Lupsasca. "The Maximally Rotating Black Hole as a Critical Point in Astronomy". PhD thesis. 2017. URL: https://dash.harvard.edu.

[12] Samuel E. Gralla, Alexandru Lupsasca, and Andrew Strominger. "Near-horizon Kerr magnetosphere". In: *Physical Review D* 93.10 (2016). DOI: 10.1103/physrevd.93.104041. URL: https://doi.org/10.1103/physrevd.93.104041.

[13] F. D. M. Haldane. ""Fractional statistics" in arbitrary dimensions: A generalization of the Pauli principle". In: *Physical Review Letters* 67.8 (1991), pp. 937–940. DOI: 10.1103/physrevlett.67.937. URL: https://doi.org/10.1103/physrevlett.67.937.

[14] Frank Wilczek and Chetan Nayak. *Exclusion Statistics: Low-Temperature Properties, Fluctuations, Duality, Applications*. 1994. DOI: 10.48550/ARXIV.COND-MAT/9405017. URL: https://arxiv.org/abs/cond-mat/9405017.

[15] A. P. Polychronakos. "Solitons and fractional statistics". In: (1995). DOI: 10.48550/ARXIV.COND-MAT/9509163. URL: https://arxiv.org/abs/cond-mat/9509163.

[16] Richard P. Feynman. *Statistical Mechanics*. CRC Press, 2018. DOI: 10.1201/9780429493034. URL: https://doi.org/10.1201/9780429493034.

[17] Roger D Thorne Kip S. Blandford. *Modern Classical Physics: Optics, Fluids, Plasmas, Elasticity, Relativity, and Statistical Physics*. Hardcover. Princeton: Princeton University Press, 2017.

[18] Yong-Shi Wu. "Statistical Distribution for Generalized Ideal Gas of Fractional-Statistics Particles". In: *Physical Review Letters* 73.7 (1994), pp. 922–925. DOI: 10.1103/physrevlett.73.922. URL: https://doi.org/10.1103/physrevlett.73.922.

[19] Takahiro Aoyama. "Specific heat of the ideal gas obeying the generalized exclusion statistics". In: (2000). DOI: 10.48550/ARXIV.COND-MAT/0005336. URL: https://arxiv.org/abs/cond-mat/0005336.

[20] Behrouz Mirza and Hosein Mohammadzadeh. "Thermodynamic geometry of fractional statistics". In: *Physical Review E* 82.3 (2010). DOI: 10.1103/physreve.82.031137. URL: https://doi.org/10.1103/physreve.82.031137.

[21] Shun-ichi Amari. *Information Geometry and Its Applications*. Springer Japan, 2016. DOI: 10.1007/978-4-431-55978-8. URL: https://doi.org/10.1007/978-4-431-55978-8.

[22] Ingemar Bengtsson and Karol Zyczkowski. *Geometry of Quantum States*. Cambridge University Press, 2006. DOI: 10.1017/cbo9780511535048. URL: https://doi.org/10.1017/cbo9780511535048.

[23] Ariel Caticha. "The basics of information geometry". In: *AIP Conference Proceedings*. AIP Publishing LLC, 2015. DOI: 10.1063/1.4905960. URL: https://doi.org/10.1063/1.4905960.

[24] H Janyszek. "Riemannian geometry and stability of thermodynamical equilibrium systems". In: *Journal of Physics A: Mathematical and General* 23.4 (1990), pp. 477–490. DOI: 10.1088/0305-4470/23/4/017. URL: https://doi.org/10.1088/0305-4470/23/4/017.

[25] Pedro Pessoa and Carlo Cafaro. "Information geometry for Fermi-Dirac and Bose-Einstein quantum statistics". In: (2021). DOI: 10.48550/ARXIV.2103.00935. URL: https://arxiv.org/abs/2103.00935.

[26] V C Aguilera-Navarro, M de Llano, and M A Solis. "Bose-Einstein condensation for general dispersion relations". In: *European Journal of Physics* 20.3 (1999), pp. 177–182. DOI: 10.1088/0143-0807/20/3/307. URL: https://doi.org/10.1088/0143-0807/20/3/307.

[27] Pedro Pessoa. "Bose-Einstein statistics for a finite number of particles". In: *Physical Review A* 104.4 (2021). DOI: 10.1103/physreva.104.043318. URL: https://doi.org/10.1103/physreva.104.043318.

[28] Pedro Pessoa. "Information geometry and Bose-Einstein condensation". In: *Chaos: An Interdisciplinary Journal of Nonlinear Science* 33.3 (2023), p. 033101. DOI: 10.1063/5.0136244. URL: https://doi.org/10.1063/5.0136244.

[29] Dorje Brody and Nicolas Rivier. "Geometrical aspects of statistical mechanics". In: *Phys. Rev. E* 51 (2 1995), pp. 1006–1011. DOI: 10.1103/PhysRevE.51.1006. URL: https://link.aps.org/doi/10.1103/PhysRevE.51.1006.

[30] M Calixto and V Aldaya. "On a curvature-statistics theorem". In: *Journal of Physics: Conference Series* 128 (2008), p. 012051. DOI: 10.1088/1742-6596/128/1/012051. URL: https://doi.org/10.1088/1742-6596/128/1/012051.

[31] Black Hole Perturbation Toolkit. *Black Hole Perturbation Toolkit*. URL: http://bhptoolkit.org.

[32] Richard P Feynman, Fernando B Morinigo, and William G Wagner. "Feynman Lectures on Gravitation". In: *European Journal of Physics* 24.3 (2003), pp. 330–330. DOI: 10.1088/0143-0807/24/3/702. URL: https://doi.org/10.1088/0143-0807/24/3/702.

[33] Kip S. Thorne, R. H. Price, and D. A. Macdonald, eds. *BLACK HOLES: THE MEMBRANE PARADIGM*. 1986. ISBN: 978-0-300-03770-8.

Appendix 1: Links to the notebooks

The Mathematica notebooks produced during this work can be found at: https://github.com/jaimeangola/jaimeangola.github.io

Appendix 2: The behavior of the anyon gas in astrophysical conditions

A.2.1. Fractional parameter as a function of curvature and temperature

Now we turn the previous problem upside down. The point of view to take is very much like in the analogy posed by one of Robertson's students, that of a person taking measurements with a ruler on a hot plate[32]. There, the temperature field would make the experimentalist, who considers this field to be homogeneous and isotropic, that is her ruler that changes as it moves between hither and yon, not realizing that it is the environment what makes the change in the trustworthy ruler. Our hot plate is the space where the gas of anyons lives. The anyons feel now the curvature and temperature of the space that hosts them and the assumption here is that they respond in the same way as they expressed curvature. As they are a lump in free motion in empty space, the fugacity is going to be considered small in this first survey.

We use the ultrarelativistic case of 3D anyons, which might fit better for quanta travelling in the target space of the vicinity of the singularity of an extreme Kerr black hole. We could have equally well used the galilean case if we consider an asymptotically flat region of interstellar media.

We are going to need $\rho = \rho(\beta, z, R)$. Deriving it from the expression for R, if given by (12) we are doomed. It would make no sense at this point to look for precision at the cost of clarity and computability so we come to the compromise of transforming R by taking as many first order series as necessary of the polylogarithm functions it contains. The result remains daunting:

$$R = \frac{2\sqrt{\pi}\beta^3 \left(Li_3(z)^3 Q_1 + 4Li_4(z)^2 Q_2 - Li_4(z)Li_3(z)^2 Q_3\right)}{\left(3Li_3(z)^2 - 4Li_2(z)Li_4(z)\right)^3} \tag{1}$$

Where we introduced Q_1, Q_2 and Q_3 for clarity, being their values:

$$Q_1 = -4\rho Li_2(z)^2 + 3(1-2\rho)Li_3(z)Li_2(z) + 12\rho Li_3(z)(Li_3(z) + (1-z)\log)$$
$$Q_{2_1} = (2-4\rho)Li_2(z)^3 - 4\rho Li_3(z)\left((1-z)\log^2\right) - 2\rho Li_2(z)^2((1-z)\log)$$
$$Q_{2_2} = Li_3(z)Li_2(z)\left((1-z)\log - \frac{4\rho(1-2z)}{\tanh}\right)$$
$$Q_3 = (10-20\rho)Li_2(z)^2 + 2\rho Li_2(z)(8Li_3(z) + 13(1-z)\log) + 3Li_3(z)\left((1-z)\log - \frac{4\rho(1-2z)}{\tanh}\right)$$

Nevertheless it allows for a numerical evaluation and this suffices for our purposes at this stage.

According to Fig. 12 non very bosonic anyons can live only in a certain range of temperature for a given a curvature that they might be exposed to, at least as long as their fugacity is kept very low ($z = 0.01$ was used). We also see that the bosonic sector is slightly favoured and curvature enhances this asymmetry. At a given fugacity or for β high, which dominates over z in most of the domain, from 12, an approximate fit can be constructed by inspection and some trial and error. For up to moderate values of curvature we can write:

$$\rho(\beta, R) = e^{-\left(\beta^{1/\beta}+\beta\right)}(R\log)\left(1 - e^{-(\beta + R\log)^2}\right) \tag{2}$$

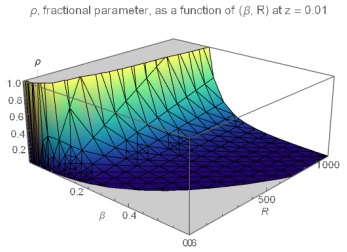

Figure 12: Fractional parameter as a function of low β and R for fugacity values $z = 0.01$ (3D ultrarelativistic) derived from (1)

But we are not done, for Fig. 12 is also saying that the fractional parameter doesn't exist for negative values of R. This contradicts what we have already witnessed all this way, these values for ρ correspond to the fermionic sector. This signals a problem with (1) and (2). After working many different alternative expressions for ρ (β, R) in terms of numerically solving for ρ (for instance taking series up to four terms of the polylogarithms recursively until only

logarithms are left and/or adding the substitution of series of the logarithms, polylogarithms at different stages, and a full fledge substitution of whatnot till arriving at a expressions for R like (3)) nothing ended up working in a reliable way. *Exempli gratia*, one such transforms tried, was:

$$R = \frac{2\sqrt{\pi}\beta^3(2\rho-1)\left(-\frac{1}{3}2\rho z^2\left(\frac{2\rho\left(z\left(z\left(4\rho^2+6\rho-\left(\left(6\rho^2+4\rho+3\right)\rho+3\right)z+9\right)-3(\rho+3)\right)+3\right)}{(z-1)^4}-3\right)+(z-2\rho z)^2+z\right)}{(z-2\rho z)^3} \tag{3}$$

Neither (1) nor (2) gives the right ρ when run against the cases studied in the previous section as a check. The results obtained by these won't be fully discarded, but they need to be taken cautiously accepting their fragility. Considering that we are interested in applying this to the specific case described in a later subsection, which requires low z, high β and up to very large absolute values of curvature, we obtained an empirical expression based on the results of the previous subsection:

$$\rho(\beta, R) = \frac{2.3244810^8 - R}{(4.6489610^8)\,\beta^3} \tag{4}$$

Withal, the physical consequence of (4) and whatever other expression obtained in a similar fashion, is that subject to a gravitational and/or temperature field, there is a natural selection of fractional parameter in terms of the background metric. In a theory of an anyonic ideal gas whose constituent particles can adjust its fractional parameter, those would transient themselves to acquire the proper values, at least collectively, while for models which keep the fractional parameter fixed, these plots represent how the different particles or clusters of them with a certain coarse-grained parameter would distribute. If no risk is wanted to be assumed, nothing in the rest of this subsection is needed for the next and last one, which deals solely with results obtained by use of (4) and could be, therefore, trusted. The main disadvantage in skipping the rest of the present one is that the interpretation of the results will be restricted to that applied case where no other value of fugacity different from 0.1 will be considered. With this in mind we proceed with our analysis.

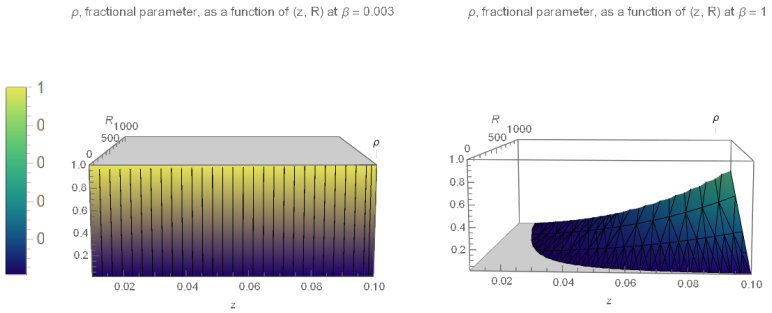

Figure 13: Fractional parameter as a function of fugacity (in its lower limit) and curvature for $\beta = 0.003$ and for $\beta = 1$ respectively (3D ultrarelativistic) using numerical evaluation for obtaining ρ by use of (2). But (2) is flawed so this results might only be qualitative (see main text for an explanation)

If terms of fugacity dependence, in the low limit, giving some validity to Fig. 13, it shows that at very low β we have a reminiscence of a fermi surface filled with mostly highly fermionic anyons and a portion of highly bosonic excitations but no intermediate fractional values, in contrast with the behavior as temperature drops, getting almost no particles from highly fermionic sector at any curvature when β is unitary (right of the figure). As fugacity increases, the excitations behave more like fermions (or only very fermionic particles are allowed, as we said). This is depicted in 14. Unavoidably, according to (2), at $z = 1$, another side of the fermi surface appears and no fractional excitations live beyond.

If we explore the full perspective of β and long range of R (always low z), we see that intermediate parameter

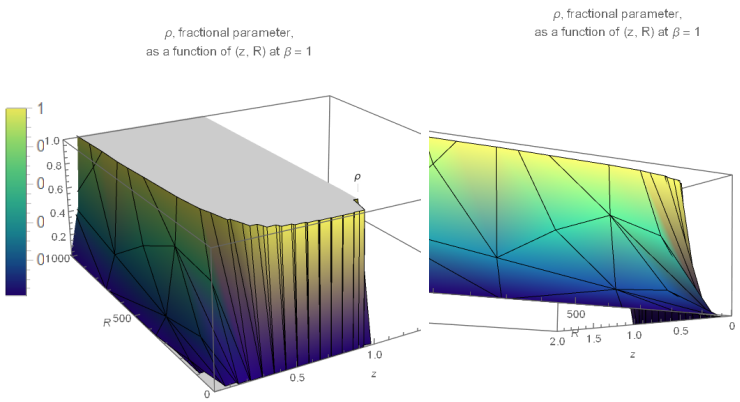

Figure 14: Fractional parameter as a function of fugacity (in its lower limit) and curvature for $\beta = 1$ (3D ultrarelativistic). These were obtained by numerical reversing (2) so results could only be qualitatively considered in the best of cases

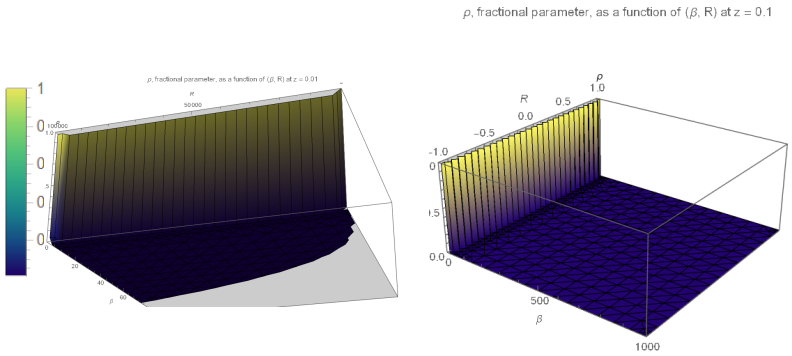

Figure 15: Fractional parameter as a function of β (in long range) and curvature (3D ultrarelativistic). Left.: obtained by numerical reversing (2) and with $z = 0.01$. Right: obtained by using (4), and thence, for $z = 0.1$. Although the two plots look very similar, a detailed inspection of the scope of R shows that the results are very different as those coming from (2) are null from flatness to negative values. Nevertheless the concordant picture for positive values of R brings some relief to the dodgy use of (2)

anyons are inhibited. We only have the fermionic sector for very low β and they do so rather insensibly to the change in R. On the other hand, as β increases, the fermionic sector vanishes completely and we are left with almost pure bosons that can condensate. This behavior is a coincident result of both (2) and (4).

When we move to lower temperatures, we observe the appearance of intermediate fractional parameter excitations occupying states reserved to almost pure fermionic or pure bosonic anyons at higher temperatures (c.ref. Fig. 13). This seems to take place predominantly close to flatness and for the lowest values of fugacity. Under this conditions highly bosonic anyons are almost absent in sharp contrast with almost all other values of the parameters.

A.2.2. Distribution of particles and internal energy for the free anyon gas from in silica approximation to $\rho(\beta, R)$

Reversing our steps we calculate both the distribution of the number of particles and the internal energy as function of curvature by plugging (4) into their expressions as given in the previous section. The results are shown in Fig. 18.

Fugacity is aside in (4), so even if this seems to be a good description not only for $z = 0.1$, (4) works accurately only there. That said, we observe that independently of number of particles a Fermi surface (in the sense described

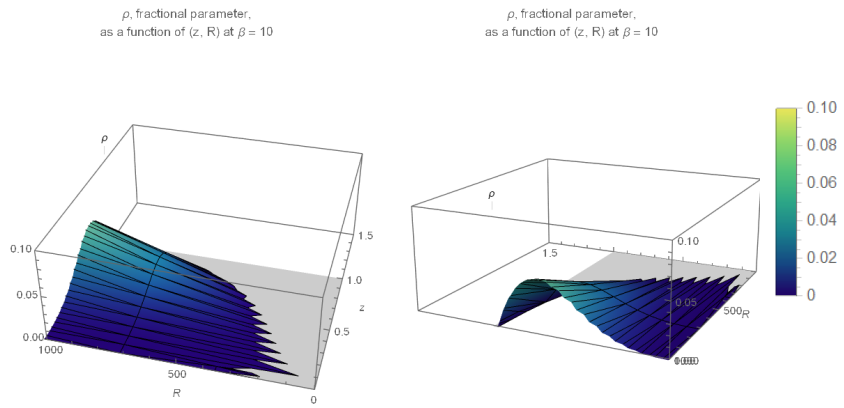

Figure 16: Fractional parameter as a function of z (in the long range) and curvature for $\beta = 10$ (3D ultrarelativistic). Fugacity was covered well beyond 1 although there are no contributions beyond that value, reason why they are not included in the captions. Carefully see that here the vertical axis (ρ value) ranges up to 0.1 only. These were obtained by numerical reversing (2) so results could only be qualitatively considered in the best of cases.

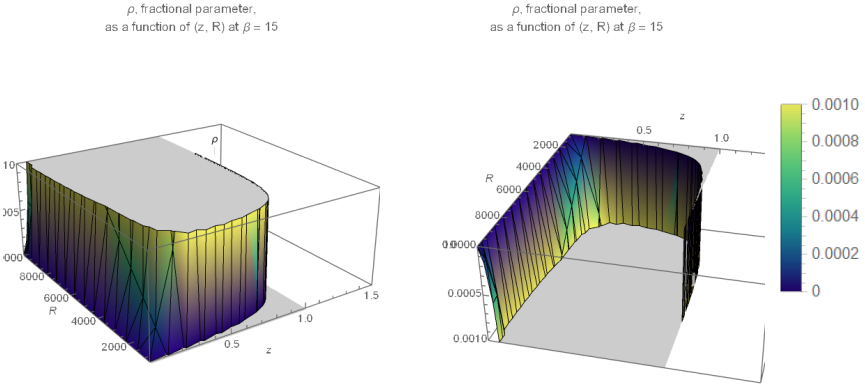

Figure 17: Fractional parameter as a function of z (in long range) and curvature for $\beta = 15$ (3D ultrarelativistic). Fugacity was covered well beyond 1 although there are no contributions past that value, reason for not including that region in the figures. See that here the vertical axis (ρ value) ranges up to 0.001 only. These were obtained by numerical reversing (2) so results could only be qualitatively considered in the best of cases

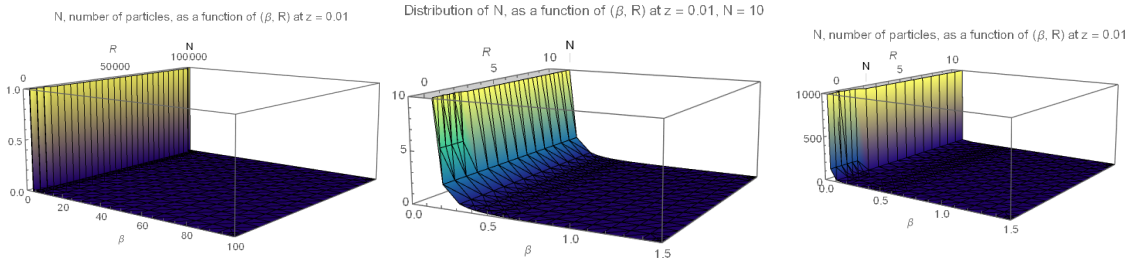

ut supra) develops at low β. For $N = 1$, where this model is not expected to be reliable, the interpretation could only be as a probability density for the anyon of occupying a particular fractional parameter if this could make any sense taking into account that we are dealing with an essentially statistical property, and it may just be a purely mathematical closure relation. Increasing the number of particles, and in all cases, for higher β we only have very

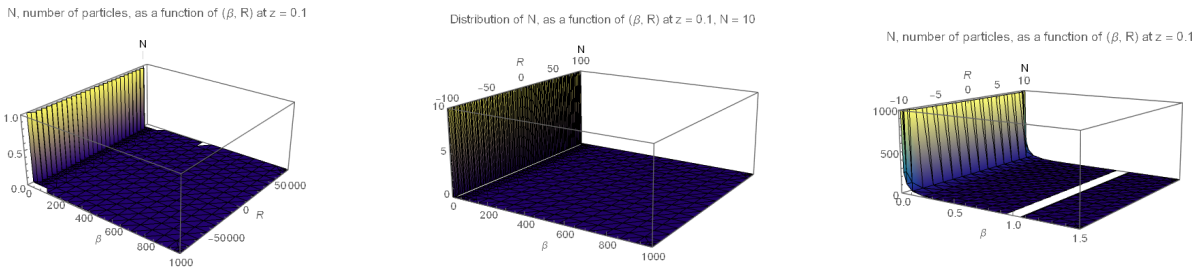

Figure 18: Distribution of the number of particles as a function of curvature and temperature at z = 0.01 for different values of N. From left to right, N = 1, N = 10, N = 1000. From (2) in the upper row, and from (4), z = 0.1, in the lower row

bosonic anyons and we see that N follows the fractional parameter. For $N > 1$ we observe, as we did in Fig. 14, that flatness allows for intermediate values of the parameter and we learn that intermediate fractional statistics can be better observed at the triple-low: low β, low curvature and low number of particles. Examined at higher fugacities the behavior does not significantly differ from the exhibited at very low fugacities. The internal energy behaves in similar fashion although the system seems to favor storing energy from highly bosonic up to moderate fermionic anyons, not so dichotomously as the number of particles, but in a more democratic way. The non-null fermionicity sector is favoured when we are at very low β, leaving the of task to the highly bosonic partners as temperature drops (Fig. 19).

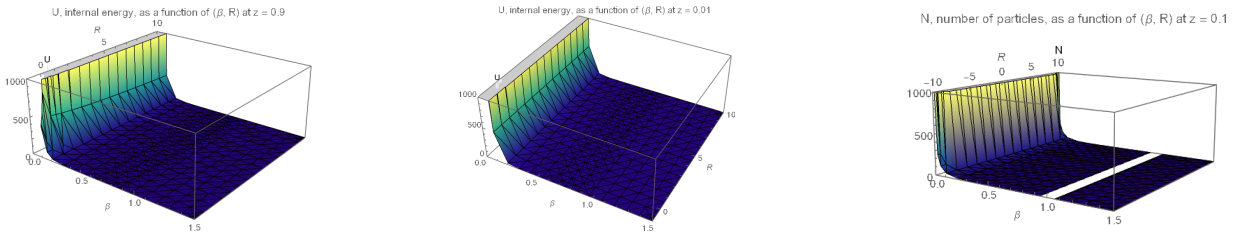

Figure 19: The internal energy as a function ofβ and R for z = 0.9 and z = 0.01. Left and center, from (2). The right picture was obtained by (4)

A.2.3. Behavior of the fractional parameter in the vicinity of the singularity of a maximally rotating black hole

As a final application we study the distribution of the fractional parameter in the vicinity of the singularity of a maximally rotating black hole. The Ricci scalar would then as depicted in Fig. 20 (actually we worked with three different values of rotation, a typical one $a \sim 0.6$, a settled one at $a \sim 0.998$ [33] and at true $a = 1$, in the usual scale for the angular momentum: $a\epsilon[0, 1]$ is so that 0 means no rotation and 1 the maximum speed achievable, c)[[4, 10, 11, 17]]. Although it may look worthless studying the behavior of the fractional parameter so close to the singularity from an astronomer perspective, as we are deep beyond the horizon, we need to remember that in Kerr geometry, as we approach $a = 1$ the throat developed emerges a symmetry along the r parameter[[10, 11]] allowing us to expect that results near the horizon it will resemble closely those infinitesimally distant from the singularity. This motivates the ensuing use of our relation for the fractional parameter on the curvatures thereof shown in the ensuing 3D plots (Fig 20).

If we want curvature to give us the easiest result to interpret in terms of the fractional parameter, this should be the character reversal of the last one. The new branches of research in the preceding sections came from answering respective questions, in the same mood, the inquiry here reveals itself as: is there a range of curvature for which the

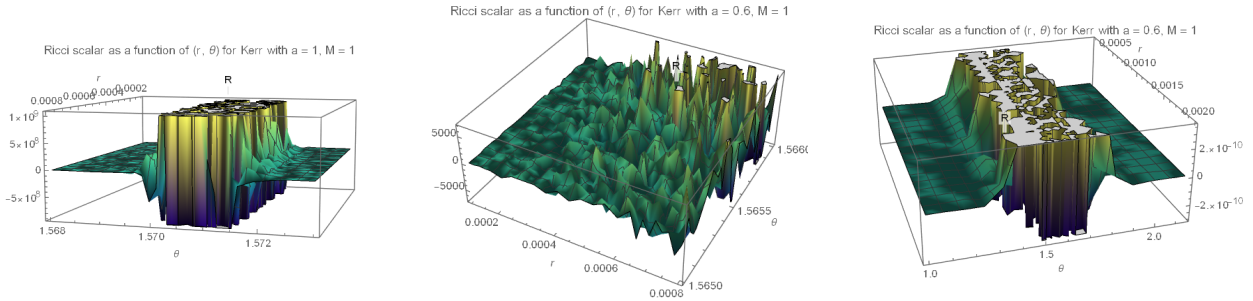

Figure 20: Left: The curvature in the vicinity of the singularity of a Kerr black hole at maximum rotation speed. Center and right: at lower angular momentum ($a = 0.6$). These were obtained using the Black Perturbation Toolkit[30]

sectors of different *fermionicity* behave in opposite way to the way we observed so far?. The answer is affirmative. Immediate use of (4) give us the requested parameter values, summarized in Table 1.

Range of curvature	β	Character
$2.31983 \times 10^8 < R < 2.32216 \times 10^8$	0.1	fermionic $(0.5 < \rho < 1)$
$-2.32448 \times 10^{14} < x < 0$	100	bosonic $(0 < \rho < 0.5)$

Table 1: Conditions at $z = 0.1$ for which the *fermionicity* of the free ideal anyon gas appears reversed compared to the cases analyzed so far. For those values of temperature and curvature, the bosonic sector is linked to negative curvatures whereas the fermionic sector is linked to positive curvatures. This cannot be considered exhaustive as only some physically plausibly ranges were combed and (4) by itself was built up to be reliable chart at the expense of covering a smaller domain

Under the conditions there presented, the relation between *fermionicity* of the sector and the curvature has flipped sign. Moreover, the ranges described by no means are exhaustive. They are obtained from (4) which is a featureless sketch of the much more complex but true (2). But even if (4) is so limited, it's not so much as not to allow these characterization reversal to bet spotted. Direct feed of the tabulated values of the first row of Table. 1 into (4) provides us with the maps for the distribution of the fractional parameter shown in Fig. 21, which on the right of the image the corresponding Ricci scalar map also plotted.

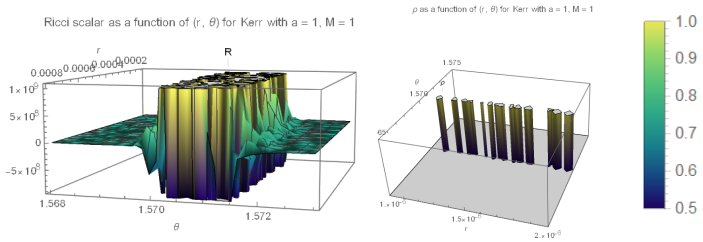

Figure 21: Left: fractional parameter in the vicinity of the singularity of a maximally rotating Kerr black hole. For z = 0.1 and $\beta = 0.1$. Contrary to what was observed in the foregoing, under these conditions, the fractional parameter presents a reversed curvature-dependency bringing the fermionic sector to positive curvatures. Right: values for the Ricci scalar over the sampled region in the left of the figure

If instead, the values of the second row of Table 1. are used we get the results shown in Fig. 22 and 23. Where for plotting purposes only the first negative slice of curvature was used R $\epsilon[0, -1]$ (right part of the figure). In this case the bosonic sector is observed in this hyperbolic geometry.

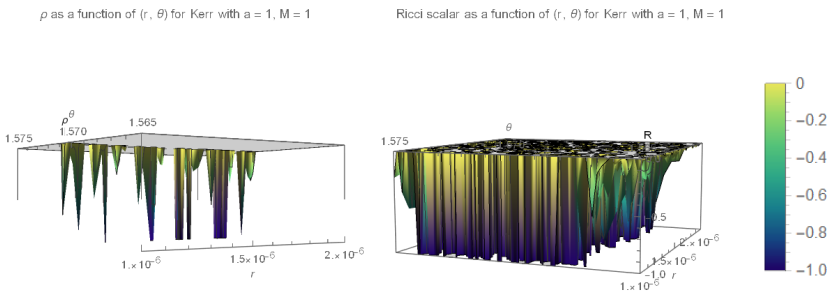

Figure 22: Fractional parameter in the vicinity of the singularity of a maximally rotating Kerr black hole. For fugacity z = 0.1. and low temperature ($\beta = 100$). Contrary to what was observed in the cases studied in the previous section, under these conditions, the fractional parameter presents a reversed curvature-dependency bringing the bosonic sector to negative curvatures. Right: values for the Ricci scalar over the sampled region in the left of the figure

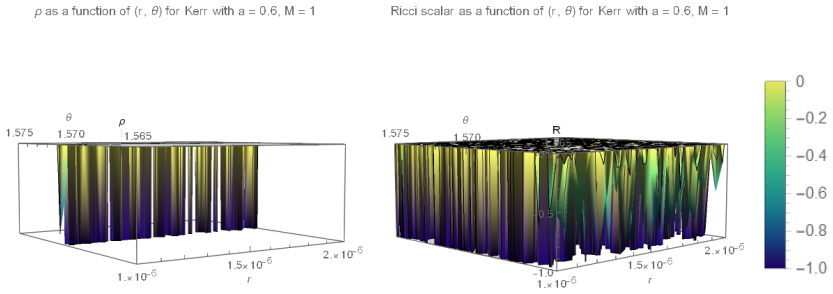

Figure 23: Fractional parameter in the vicinity of the singularity of a typically observed rotating Kerr black hole at slightly above half the maximal rotational speed (a = 0.6). For fugacity z = 0.1 and low temperature ($\beta = 100$). Contrary to what was observed in the foregoing, under these conditions, the fractional parameter presents a reversed curvature-dependency bringing the bosonic sector to negative curvatures and the fermionic sector to positive ones (for this last see notebook). Right: values for the Ricci scalar over the sampled region in the left of the figure

Appendix 3: Derivation of the correction term for Gentile's statistics

Here you find the derivation of the correction term for Gentile's statistics.
Let us assume the Gentile statistics (up to p particles per quantum state). The partition function for the gran canonical ensemble is:

$$Z = \sum_x \prod_i (e^{-\lambda 1 \epsilon_i} e^{-\lambda 2})^{x_i} \tag{1}$$

Writing this more explicitly and applying the distributive property we have:

$$Z = \prod_i [\sum_{x_i=0}^{p} (e^{-\lambda 1 \epsilon_i} e^{-\lambda 2})^{x_i}] \tag{2}$$

which is a geometric progression sum yielding:

$$Z = \prod_i \frac{1 - \left(e^{-\lambda 1 \epsilon_i} e^{-\lambda 2}\right)^{p+1}}{1 - e^{-\lambda 1 \epsilon_i} e^{-\lambda 2}} \tag{3}$$

Note that for $p = 1$ we have:

$$Z = \prod_i \frac{1 - \left(e^{-\lambda 1 \epsilon_i} e^{-\lambda 2}\right)^{2}}{1 - e^{-\lambda 1 \epsilon_i} e^{-\lambda 2}} = \prod_i \left(1 + e^{-\lambda 1 \epsilon_i} e^{-\lambda 2}\right) \tag{4}$$

While for p $\to \infty$ we have:

$$Z = \prod_i \frac{1}{1 - e^{-\lambda 1 \epsilon_i} e^{-\lambda 2}} \tag{5}$$

Now, if we find N from Z in (1) we have:

$$N = -\frac{\partial LogZ}{\partial \lambda 2} = -\sum_i \left\{ \frac{-p\left(e^{-\lambda 1 \epsilon_i} e^{-\lambda 2}\right)^{p+1} + (p+1)\left(e^{-\lambda 1 \epsilon_i} e^{-\lambda 2}\right)^{p} - 1}{\left[e^{-\lambda 1 \epsilon_i} e^{-\lambda 2} - 1\right]\left[\left(e^{-\lambda 1 \epsilon_i} e^{-\lambda 2}\right)^{p+1} - 1\right]} \right\} \frac{\partial \left(e^{-\lambda 1 \epsilon_i} e^{-\lambda 2}\right)}{\partial \lambda 2} \tag{6}$$

Which in the ground state becomes:

$$N_0 = -\frac{\partial LogZ}{\partial \lambda 2} = -\left\{ \frac{(p+1)\xi^p - p\xi^{p+1} - 1}{[\xi - 1]\left[\xi^{p+1} - 1\right]} \right\} \xi \tag{7}$$

Which should be the ground state correction.

$$N_0 = -\frac{\xi}{\xi - 1} = \frac{1}{\frac{1}{\xi} - 1} \tag{8}$$